Cell Reports, Volume *31*

Supplemental Information

Mechanism of Virus Attenuation by Codon Pair Deoptimization

Nicole Groenke, Jakob Trimpert, Sophie Merz, Andelé M. Conradie, Emanuel Wyler, Hongwei Zhang, Orsalia-Georgia Hazapis, Sebastian Rausch, Markus Landthaler, Nikolaus Osterrieder, and Dusan Kunec

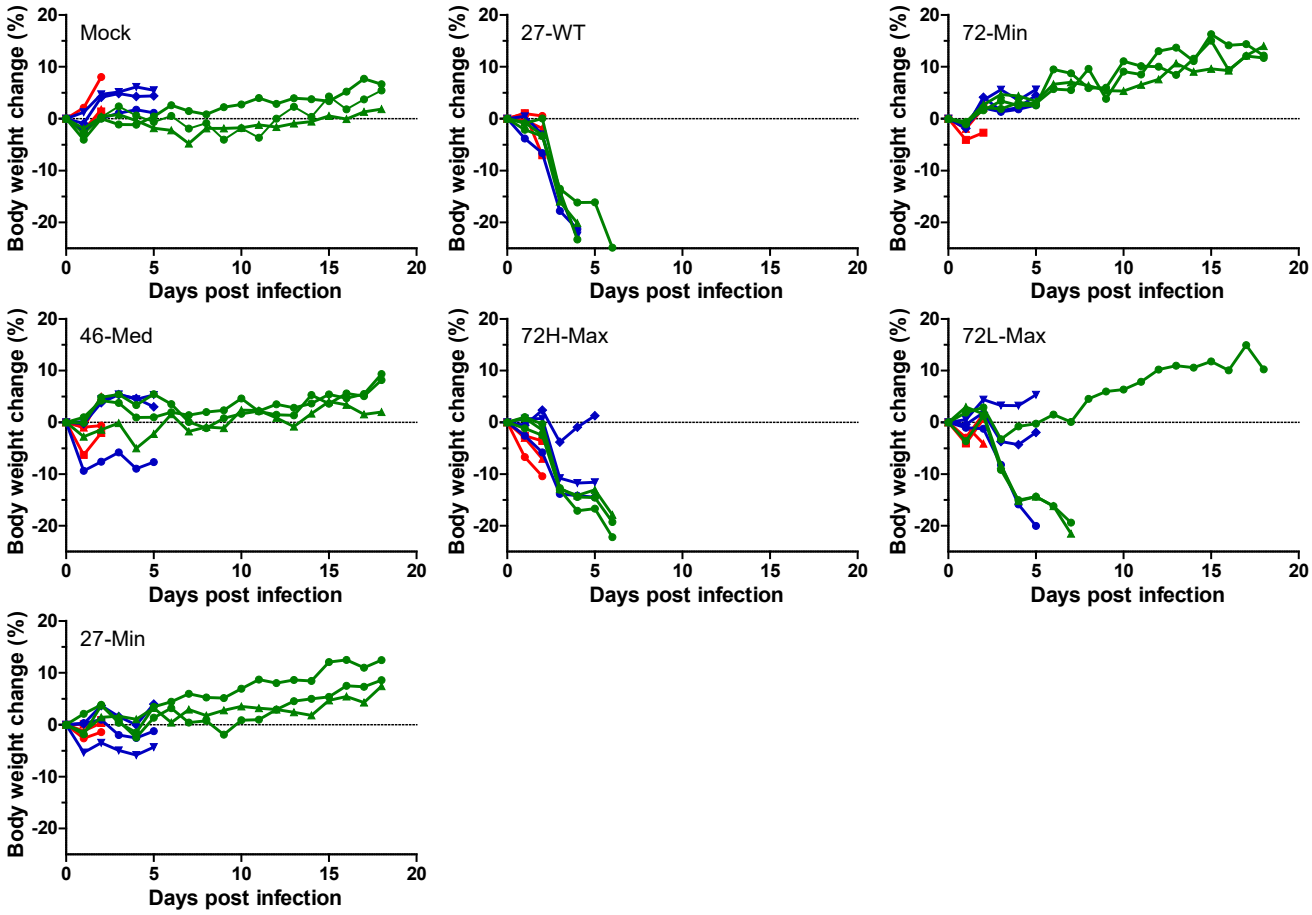

Figure S1. Survival and body weight changes of individual mice after infection with IAV, related to Figure 3A. Nine 6-week-old BALB/c mice were infected with the parental or recoded IAV or DMEM as control. On day 2 (red), 5 (blue) and 18 (green), three animals of each group were euthanized. Mice in moribund conditions, or those which lost more than 20 % body weight were euthanized earlier than scheduled.

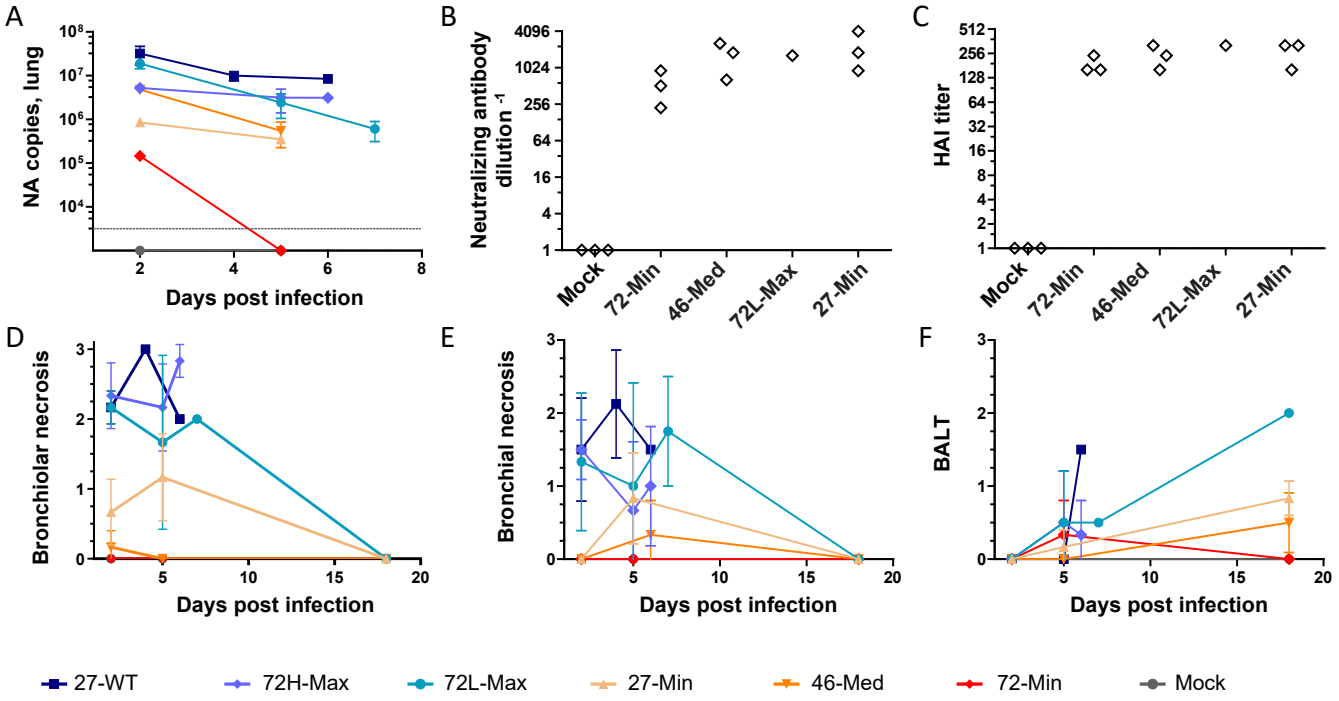

Figure S2. Histopathological changes in the lungs of infected mice, related to Figure 3. Nine 6-week-old BALB/c mice were infected with different recoded influenza viruses. On day 2, 5 and 18 three animals were euthanized or earlier if they lost more than 20 % body weight. (**A**) The right lung lobes were homogenized and copy numbers of NA segment were determined. Data are represented as mean ± SD. No virus could be detected in samples on day 18. (**B**) Anti-IAV neutralizing antibody titers were measured and (**C**) an HAI test was performed at 18 dpi with serum of mice. (**D-F**) Left lung lobes were embedded in paraffin, cut into sections, and lesions were scored from 0 (no lesion) to 3 (severe lesions). 27-WT, 72H-Max and 72L-Max show marked (**D**) bronchiolar necrosis, (**E**) bronchial necrosis and (**F**) mild increase in bronchus-associated lymphoid tissue (BALT), 72-Min, 46-Med and 27-Min only moderate or none. Data are represented as mean ± SD.

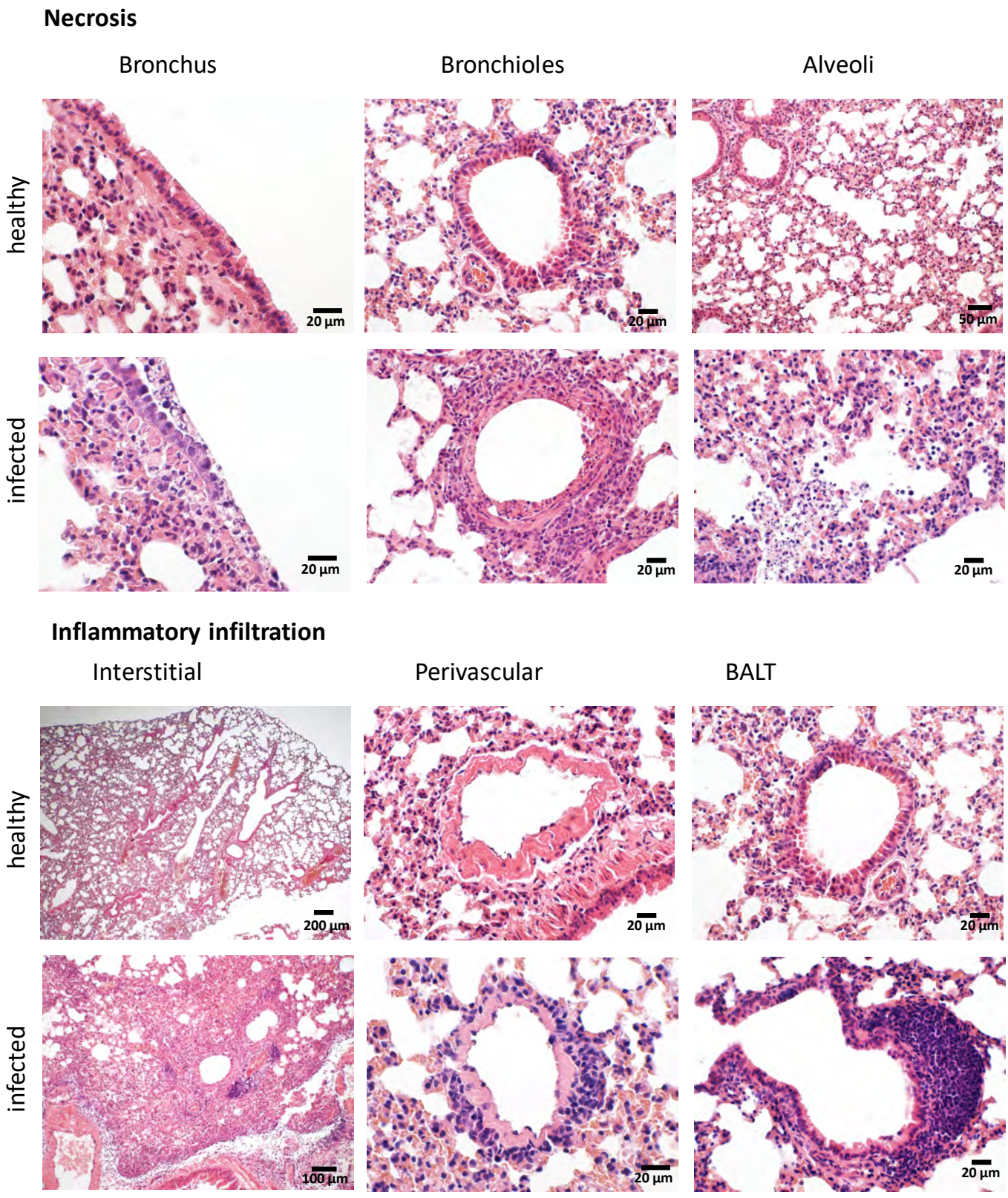

Figure S3. Representative images of histopathological changes that were assessed in the lungs of infected mice, related to Figure 3. To assess the distribution and character of pathologic changes in the lungs of infected mice, lung sections were stained with hematoxylin and eosin and microscopically evaluated for necrosis (bronchi, bronchioli and alveoli) and inflammation (perivascular, interstitial, bronchus-associated lymphoid tissue (BALT)). Representative tissue sections of healthy and infected lungs are shown.

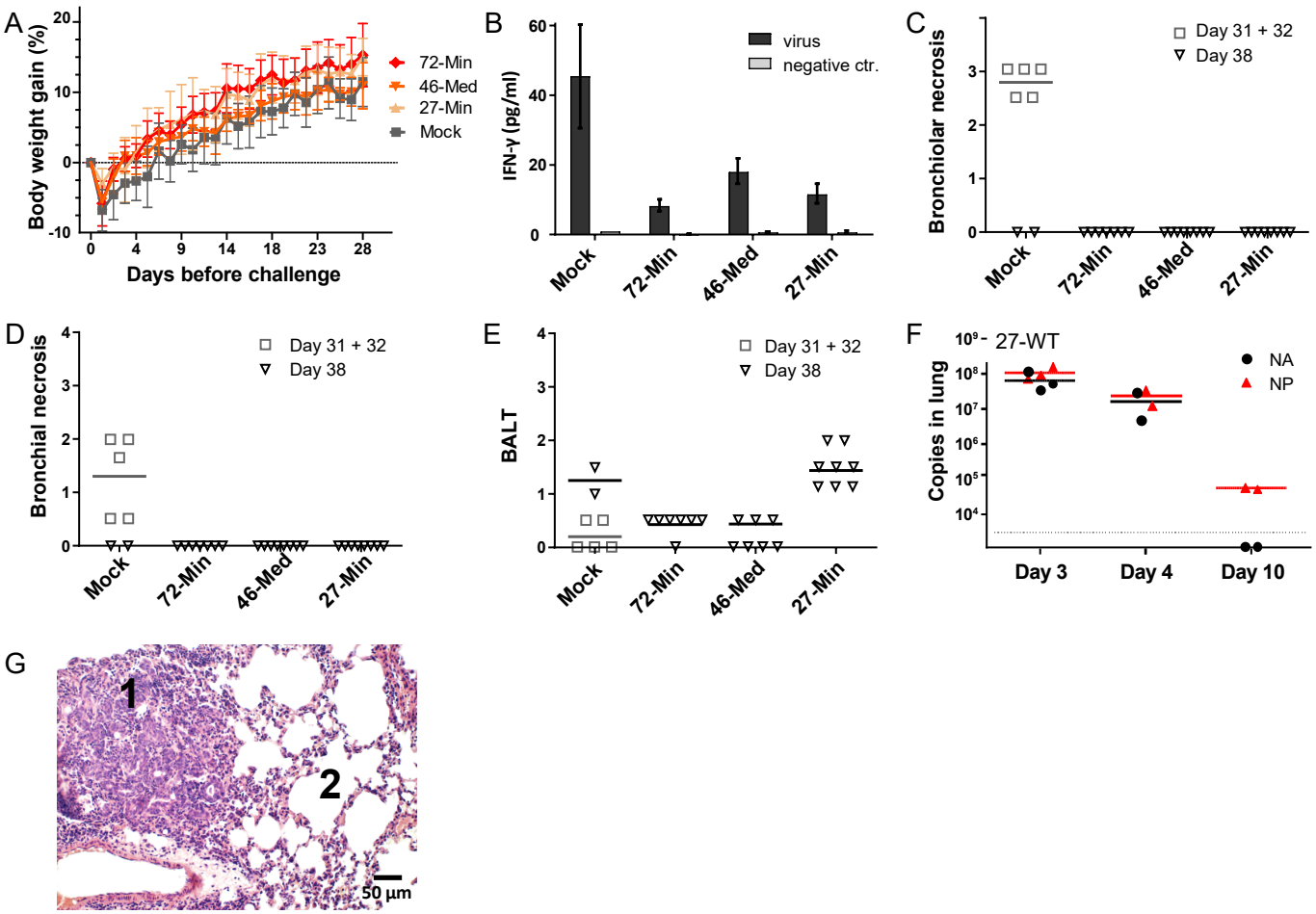

Figure S4. Histopathological assessment of the severity and distribution of pneumonic lesions in the lungs of immunized mice, related to Figure 4. Eight six-week-old BALB/c mice were vaccinated with attenuated viruses and one control group was inoculated with DMEM. (**A**) All groups showed similar development of body weight after vaccination. Data are represented as mean ± SD. (**B**) Production of IFN-γ by splenocytes. Mouse splenocytes were isolated 10 days after challenge, stimulated with purified IAV virus or control protein for 3 days, and production of IFN-γ was measured by ELISA. Data are represented as mean ± SD. (**C-E**) Left lung lobes were embedded in paraffin, cut into sections and lesions were scored from 0 (no lesions) to 3 (severe lesions). Shown are (**C**) bronchiolar necrosis, (**D**) bronchial necrosis and (**E**) bronchus-associated lymphoid tissue. (**F**) Number of NA and NP copies of mock-vaccinated mice are shown after challenge. (**G**) Image of pneumocyte type II hyperplasia (repair) of with hematoxylin and eosin stained in paraffin embedded lung. The left side of the image shows affected (1) and the right side unaffected tissue (2).

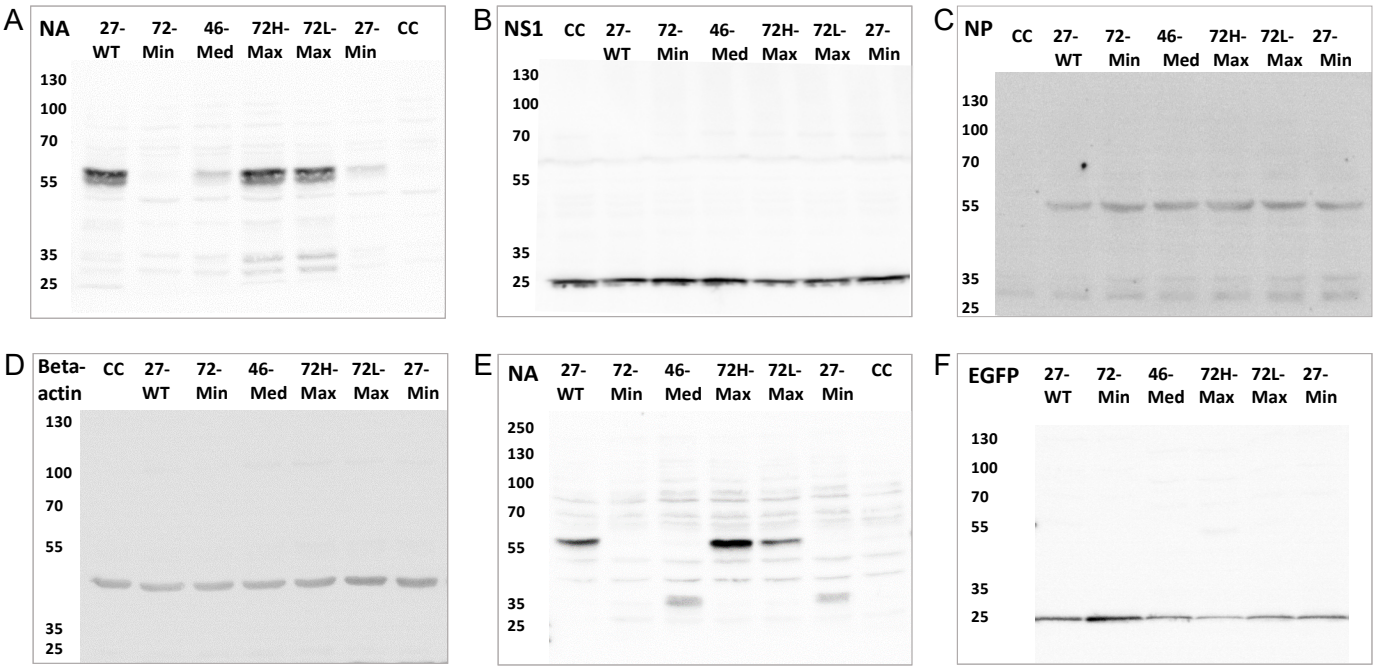

Figure S5. Uncropped images of western blots shown in the manuscript, related to Figure 2 and Figure 5. (**A-D**) Images of western blots from Figure 2F. MDCK cells were infected with the parental and recoded viruses for 5 h and the production of NA (**A**) NS1 (**B**), NP (**C**) and beta-actin (**D**) proteins was analyzed by western blotting. (**E, F**) Images of western blots from Figure 5B. HEK 293T cells were transfected with expression plasmids pVITRO2-EGFP-NA for 24 h and the production of NA (**E**) and EGFP (**F**) proteins was detected by western blotting.

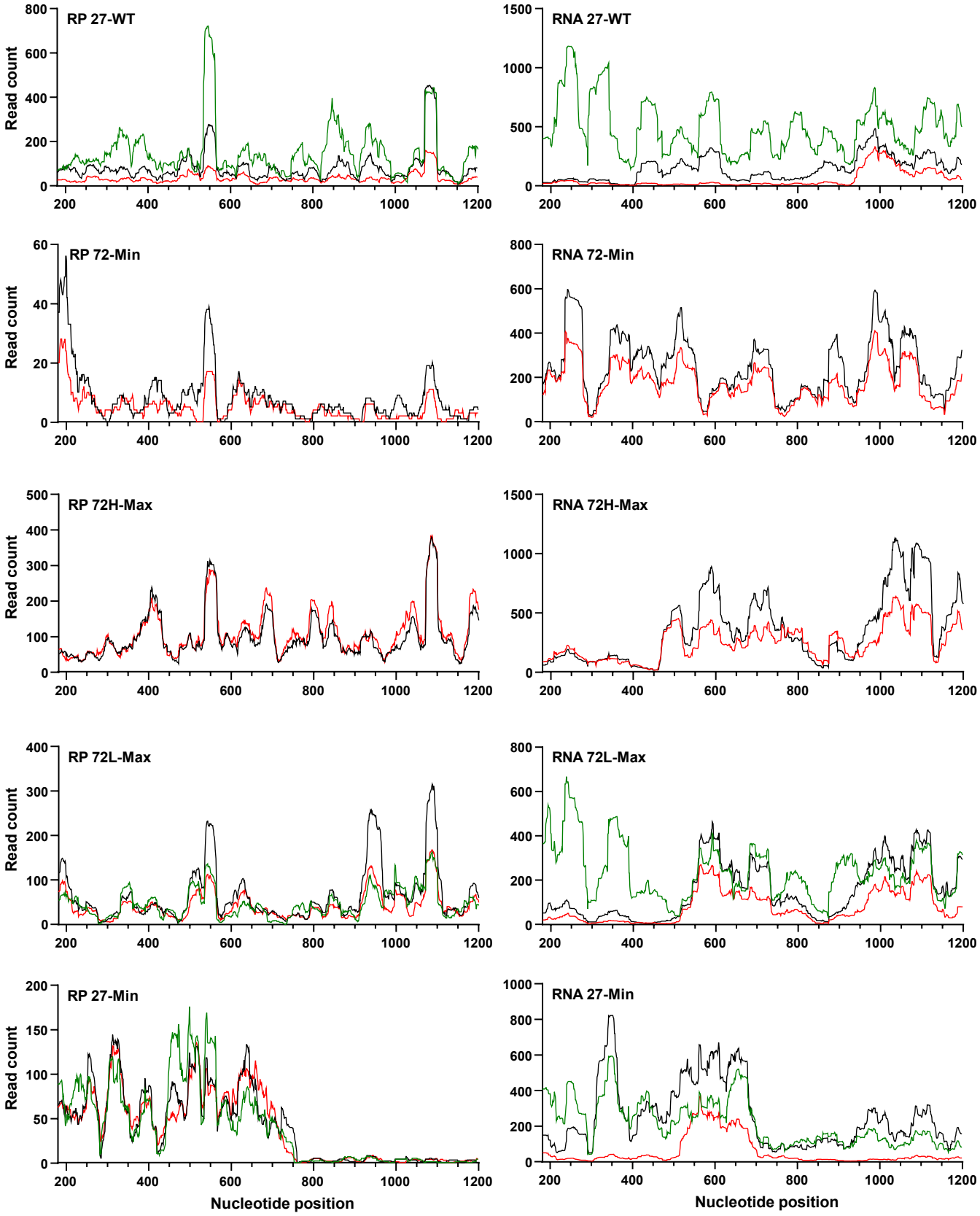

Figure S6. Read density of ribosome footprints and total RNA by next generation sequencing from recoded parts of NA fragments in transiently transfected cells, related to Figure 5. Red, black and green read densities represent replicates.

Table S1. Primers and probes for RT-qPCR, related to Figure 5 and STAR Methods

Name	**Sequence 5'-3'**
NA 3' end forward	CTGGACTAGTGGGAGCATCA
NA 3' end reverse	ATGGTGAACGGCAACTCAG
NA 3' end probe	6-FAM-CACCGTCTGGCCAAGACCAATC-TAMRA
NA 5' end forward	TGGGTCAATCTGTATGGTAGTC
NA 5' end reverse	GCTGCCTTGGTTGCATATT
NA 5' end probe	6-FAM-TGGATTAGCCATTCAATTCAAACCGGA-Tamra
EGFP forward	CCACAAGTTCAGCGTGTCC
EGFP reverse	GAACTTCAGGGTCAGCTTGC
EGFP probe	6-FAM-TGGCATCGCCCTCGCCCTCG-TAMRA
NP forward	CCAAAGGCACCAAACGATCT
NP reverse	AGTGGCATTCTGGCGTTCTC
NP probe	6-FAM-ACGAACAGATGGAGACTG-TAMRA